Effects of anisotropy on pattern formation in wetland ecosystems

Yiwei Cheng,[1] Marc Stieglitz,[1,2] Greg Turk,[3] and Victor Engel[4]

Received 5 November 2010; revised 22 December 2010; accepted 3 January 2011; published 23 February 2011.

[1] Wetland ecosystems are often characterized by distinct vegetation patterns. Various mechanisms have been proposed to explain the formation of these patterns; including spatially variable peat accumulation and water ponding. Recently, short-range facilitation and long-range competition for resources (a.k.a scale dependent feedback) has been proposed as a possible mechanism for pattern formation in wetland ecosystems. We modify an existing, spatially explicit, advection-reaction-diffusion model to include for a regional hydraulic gradient and effective anisotropy in hydraulic conductivity. This effective anisotropic hydraulic conductivity implicitly represents the effect of ponding: a reduction in the long-range inhibition of vegetation growth in the direction perpendicular to the prevailing hydraulic gradient. We demonstrate that by accounting for effective anisotropy in a simple modeling framework that encompasses only a scale dependent feedback between biomass and nutrient flow, we can reproduce the various vegetation patterns observed in wetland ecosystems: maze, and vegetation bands both perpendicular and parallel to prevailing flow directions. We examine the behavior of this model over a range of plant transpiration rates and regional hydraulic gradients. Results show that by accounting for the effective *x*-*y* anisotropy that results from biomass-water interaction (i.e., ponding) we can better understand the mechanisms that drive ecosystem patterning. **Citation:** Cheng, Y., M. Stieglitz, G. Turk, and V. Engel (2011), Effects of anisotropy on pattern formation in wetland ecosystems, *Geophys. Res. Lett.*, *38*, L04402, doi:10.1029/2010GL046091.

1. Introduction

[2] Wetland ecosystems are often characterized by vegetation patterns. For instance, maze patterns are commonly observed in northern bogs. These patterns consist of interconnected hummock forming ridges that are slightly elevated above wetter hollows. Another pattern characteristic of the northern bogs is the string pattern [*Sakaguchi*, 1980; *Foster et al.*, 1983], which consists of elevated vegetation bands that are orientated perpendicular to the water flow direction and which are separated by waterlogged sloughs (hereafter this type of pattern will be referred to as *perpendicular strings*). Vegetation bands orientated parallel to the prevailing flow direction have also been observed in wetland ecosystems [*Ellery et al.*, 2003; *Ogden.*, 2005; *San José et al.*, 2001] (hereafter this type of pattern will be referred to as *parallel strings*). The ridge and slough ecosystem of the Florida Everglades is one such example of a parallel string pattern.

[3] A number of conceptual and simulation models have been proposed to explain the formation of maze and string patterns in wetland ecosystems [*Swanson and Grigal*, 1988; *Hilbert et al.*, 2000; *Rietkerk et al.*, 2004; *Eppinga et al.*, 2009; *Larsen and Harvey*, 2011]. For example, *Hilbert et al.* [2000] invoked a peat accumulation mechanism to explain the formation of maze patterns on flat ground. The Hilbert model describes the interaction between peat production and depth to water table. At sites where the peat surface is sufficiently above the water table, vegetation growth is near optimal, the rate of organic matter input into the soil is higher than the rate of decomposition, and thus peat accumulates. On the other hand, at saturated sites, vegetation growth is limited, the rate of organic matter input into the soil is lower than the rate of decomposition, and thus peat depth decreases. With time, sites with moderate soil wetness connect and form maze-like structures that surround waterlogged hollows.

[4] A ponding mechanism has been invoked to explain the development of perpendicular strings [*Swanson and Grigal*, 1988] in bogs. Specifically, a vegetation patch impedes the downslope flow of water. This then leads to ponding of upslope water, which locally increases hydroperiod and water depth and which can inhibits the upslope expansion of emergent vegetation. At a distance further upslope the water surface is lower which provides favorable conditions for patch growth. At the same time that the alternating conditions lead to growth or inhibition along the hydrologic gradient, individual patches may expand in the direction perpendicular to the hydrologic gradient. Together, these processes ultimately yield strings of vegetation perpendicular to the prevailing flow.

[5] Nutrient accumulation has also been proposed as a mechanism for vegetation pattern formation [*Rietkerk et al.*, 2004]. *Rietkerk et al.* [2004] developed a spatially explicit, advection-reaction-diffusion type model (henceforth called the Rietkerk model) to describe the formation of maze and perpendicular string patterns. Specifically, a scale dependent feedback between the plant biomass, transpiration and nutrient accumulation drives the formation of the vegetation patterns. Vegetation induces subsurface water and nutrient fluxes towards itself through transpiration, activating further growth, which increases transpiration and nutrient accumulation. In this positive feedback, the plants function as activators that promote additional growth within short distances, leading to patches of relatively higher vegetation densities than the surrounding environment (short distance facilitation). The nutrient accumulation caused by plant growth also acts as an inhibitor of growth at a distance by depleting the available nutrients for other plants or patches (long distance inhibition).

[6] We propose a modeling perspective that retains the simplicity of the original Rietkerk model, yet that reproduces

[1]School of Civil and Environmental Engineering, Georgia Institute of Technology, Atlanta, Georgia, USA.
[2]School of Earth Atmospheric Sciences, Georgia Institute of Technology, Atlanta, Georgia, USA.
[3]School of Interactive Computing, Georgia Institute of Technology, Atlanta, Georgia, USA.
[4]South Florida Natural Resources Center, Everglades National Park, Homestead, Florida, USA.

0094-8276/11/2010GL046091

Table 1. Model Parameters and Values Used to Generate Maze Pattern, String Pattern and Vegetation Bands Parallel to Flow Direction[a]

Symbol	Interpretation	Unit	Value
g	Plant growth parameter	$m^3\ g_N^{-1}\ day^{-1}$	5.48×10^{-4}
μ	Plant uptake parameter	$m^3\ g_B^{-1}\ day^{-1}$	5.48×10^{-6}
d	Recycling parameter	day^{-1}	2.74×10^{-4}
b	Plant loss parameter	day^{-1}	5.48×10^{-4}
D_B	Diffusion coefficient for biomass	$m^2\ day^{-1}$	5.48×10^{-3}
p	Precipitation	$m\ day^{-1}$	1.37×10^{-3}
t_v	Plant transpiration parameter	$m^3\ g_B^{-1}\ day^{-1}$	1.4×10^{-5}
e	Evaporation parameter	$m\ day^{-1}$	8.22×10^{-4}
k	Hydraulic conductivity	$m\ day^{-1}$	1.37
N_{in}	Nutrient input	$g_N^{-1}\ m^{-2}\ day^{-1}$	4.1×10^{-3}
r	Nutrient loss parameter	day^{-1}	2.74×10^{-4}
D_N	Diffusion coefficient for nutrient	$m^2\ day^{-1}$	2.74×10^{-2}

[a]Parameter values from *Rietkerk et al.* [2004].

the various vegetation patterns observed in wetland ecosystems. Specifically, we represent the effect of the ponding mechanism as proposed by *Swanson and Grigal* [1988], i.e., reduction of long-range inhibition in the direction perpendicular to the prevailing hydraulic gradient, implicitly through an effective anisotropy in hydraulic conductivity. We modify the Rietkerk model to include for this term. In this work, we first demonstrate that the modified Rietkerk model is able to reproduce the various patterns. Next, we examine the behavior of this model across a range of plant transpiration rates, regional hydraulic gradients, and degree of anisotropy in the effective lateral (x-y coordinate) hydraulic conductivities, to increase our understanding of the controls that govern that the evolution of vegetation patterns in wetland ecosystems. Results demonstrate the importance of the relative magnitude of the x-y advection rates on pattern formation in wetland ecosystems.

2. Method

[7] The Rietkerk model describes the dynamics of three state variables in x and y direction: vascular plant biomass (B), hydraulic head (H) and nutrient concentration in groundwater (N).

$$\underbrace{\frac{\partial B}{\partial t}}_{(\mathbf{B1})} = \underbrace{g \cdot [N] \cdot B \cdot f[h(H)]}_{(\mathbf{B1})} - \underbrace{d \cdot B}_{(\mathbf{B2})} - \underbrace{b \cdot B}_{(\mathbf{B3})} + \underbrace{D_B \cdot \left[\frac{\partial^2 B}{\partial x^2} + \frac{\partial^2 B}{\partial y^2}\right]}_{(\mathbf{B4})} \tag{1}$$

$$\underbrace{\frac{\partial H}{\partial t}}_{(\mathbf{H1})} = \underbrace{\frac{p}{\theta}}_{(\mathbf{H1})} - \underbrace{\frac{t_v \cdot B \cdot f[h(H)]}{\theta}}_{(\mathbf{H2})} - \underbrace{\frac{e \cdot f[h(H)]}{\theta}}_{(\mathbf{H3})} + \underbrace{\frac{k}{\theta} \cdot \left[\frac{\partial}{\partial x}\left(H \cdot \frac{\partial H}{\partial x}\right) + \frac{\partial}{\partial y}\left(H \cdot \frac{\partial H}{\partial y}\right)\right]}_{(\mathbf{H4})} \tag{2}$$

$$\frac{\partial [N]}{\partial t} = \underbrace{\frac{N_i - \mu \cdot [N] \cdot B \cdot f[h(H)] + d \cdot \left(\frac{\mu}{g}\right) \cdot B - r \cdot N - [N] \cdot \theta \cdot \frac{\partial H}{\partial t}}{H \cdot \theta}}_{(\mathbf{N1})} + \underbrace{D_N \cdot \left[\frac{\partial^2 [N]}{\partial x^2} + \frac{\partial^2 [N]}{\partial y^2}\right]}_{(\mathbf{N2})} + \underbrace{\frac{k}{\theta} \cdot \left[\frac{\partial}{\partial x} \cdot \left([N] \cdot \frac{\partial H}{\partial x}\right) + \frac{\partial}{\partial y} \cdot \left([N] \cdot \frac{\partial H}{\partial y}\right)\right]}_{(\mathbf{N3})} \tag{3}$$

Term B1 describes plant growth, which is nutrient limited and increases linearly with increasing plant nutrient uptake. Plant growth is also affected by water stress. The soil water stress function $f[h(H)]$ ranges from zero to unity and is a function of the pressure head, h. Pressure head is calculated as the difference between hydraulic head, H, and elevation head, z. B2 represents fraction of dead biomass that is returned to litter while B3 represents the fraction of dead biomass that is lost from the ecosystem. B4 describes the lateral spread of biomass by diffusion. H1 represents the increase in hydraulic head due to local precipitation, while H2 and H3 represent decrease in hydraulic head due to plant transpiration and evaporation respectively. H4 describes the advection of hydraulic head according to Darcy's Law. N1 describes the rate of change of nutrient availability due to anthropogenic input, uptake by plants, recycling of dead plant material and nutrient losses. N2 is the rate of Fickian diffusion of the dissolved nutrients while N3 is the advection of dissolved nutrients by groundwater flow.

[8] Equations (2) and (3) of the Rietkerk model are modified to allow for constant advection of water and nutrients in the y-direction due to a regional hydraulic gradient. After modification, terms H4 of equation (2) and N3 of equation (3) take the following forms:

$$\mathbf{H4:}\quad \frac{k_x}{\theta} \cdot \left[\frac{\partial}{\partial x}\left(H \cdot \frac{\partial H}{\partial x}\right)\right] + \frac{k_y}{\theta} \cdot \left[\frac{\partial}{\partial y}\left(H \cdot \frac{\partial H}{\partial y} + H \cdot \frac{\partial c}{\partial y}\right)\right]$$

$$\mathbf{N3:}\quad \frac{k_x}{\theta} \cdot \left[\frac{\partial}{\partial x} \cdot \left([N] \cdot \frac{\partial H}{\partial x}\right)\right] + \frac{k_y}{\theta} \cdot \left[\frac{\partial}{\partial y} \cdot \left([N] \cdot \frac{\partial H}{\partial y} + [N] \cdot \frac{\partial c}{\partial y}\right)\right]$$

Where $\partial c/\partial y$ is the regional hydraulic gradient in the y-direction. Therefore dc/dy indicates the change of hydraulic head (dc) between two adjacent grid cells of size, dy. In this scheme, the regional hydraulic gradient is identical to the land-surface slope. The values of regional hydraulic gradient are constrained to below 0.03 to maintain consistency with observed values. *Belyea* [2007] has shown that surface gradients in northern peatlands can range from 0 to 0.03 m m^{-1}. k_x and k_y (m day^{-1}) represent the hydraulic conductivity of peat in x and y directions, respectively. k_x/k_y represents the degree of anisotropy in the hydraulic conductivities and ranges from 0–1. When $k_x/k_y = 1$, the soil is isotropic.

[9] We retain the original parameter values (Table 1), and the initial and boundary conditions employed by *Rietkerk et al.* [2004]. To simulate a maze pattern on flat ground, we set $dc = 0$ m, and $k_x/k_y = 1$. To simulate perpendicular string patterns, we set $dc = 0.015$ m to simulate moderate regional hydraulic gradient and introduce anisotropic hydraulic conductivity by setting $k_x/k_y = 0.75$. To simulate parallel string, we retain a similar degree of anisotropy in hydraulic conductivity and set $k_x/k_y = 0.75$. However, the magnitude of the regional hydraulic gradient is increased and $dc = 0.025$ m.

[10] Sensitivity analysis on pertinent hydrologic parameters of the model is conducted by performing two sets of simulations to study sequences of vegetation states that accompany gradual changes in plant transpiration rate, regional hydraulic gradient that is oriented in the y-direction and degree of anisotropy in hydraulic conductivity. The first set of simulations demonstrates how changes in plant transpiration and regional hydraulic gradient affect vegetation patterning. The main parameters varied are the plant tran-

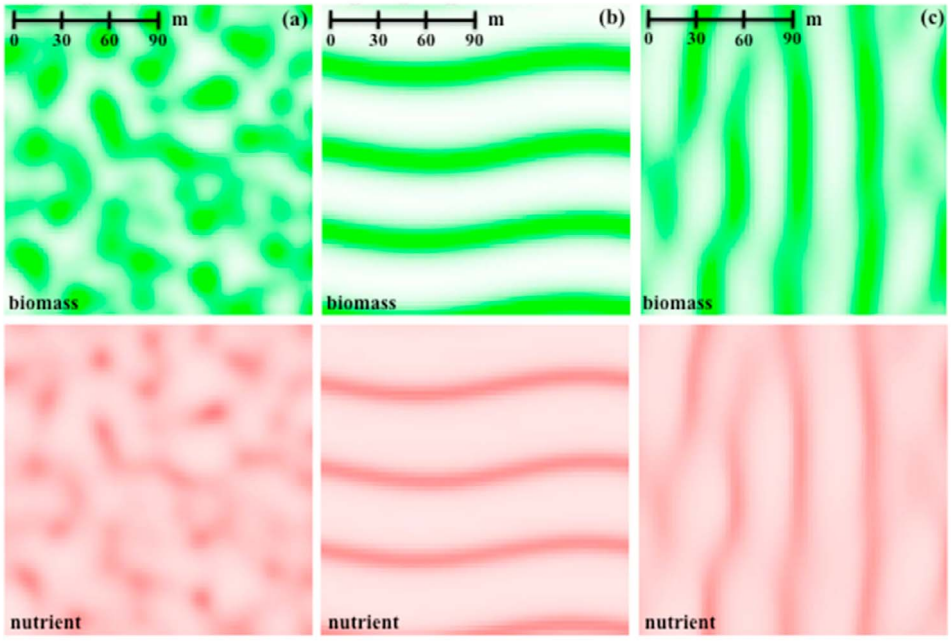

Figure 1. Simulated vegetation patterns. (a) Maze pattern on flat ground. (b) String pattern on slope. (c) Vegetation bands parallel to prevailing flow direction.

spiration parameter, t_v, and dc. t_v varies between 50% and 200% of 1.4×10^{-5} m^3 g$_B^{-1}$ day^{-1} (a value used in the earlier simulations following *Rietkerk et al.* [2004]). dc varies from 0 to 0.025 m. The second set of simulations demonstrates the interactive effects of anisotropic hydraulic conductivity and regional hydraulic gradient on vegetation patterns. The main parameters of interest are k_x/k_y and dc, which are gradually increased from 0 to 1 and 0 to 0.025 m, respectively. t_v is kept constant at 1.4×10^{-5} m^3 g$_B^{-1}$ day^{-1}.

3. Results

[11] Modeling results show that in the absence of a regional hydraulic gradient (i.e., dc = 0), a maze pattern develops with time (Figure 1a). In the presence of a moderate regional hydraulic gradient and when $k_x/k_y < 1$, the vegetation patches aggregate and spread in the direction perpendicular of the downhill flow, leading to the formation of the perpendicular string pattern (Figure 1b). However, in the presence of a larger regional hydraulic gradient, vegetation patches aggregate and spread in the direction of the downhill flow, leading to the formation of regular vegetated bands oriented parallel to the flow direction (Figure 1c). For all three vegetation patterns, the spatial distribution of dissolved nutrient matches the distribution of biomass.

[12] Figure 2a shows the resulting vegetation states from the sensitivity analysis of plant transpiration rate and regional hydraulic gradient (selected results shown). The model predicts homogenous distribution of plant biomass at a low plant transpiration rate of $t_v = 0.7 \times 10^{-5}$ m^3 g$_B^{-1}$ day^{-1}, independent of c (Figure 2a, first row). In the absence of a regional hydraulic gradient, as plant transpiration rate increases, maze patterns form first, then patch patterns start to emerge. (Figure 2a, first column). In the presence of a large regional hydraulic gradient (dc = 0.025 m), and as plant transpiration rate increases, parallel strings start to form. As t_v continues to increase, the distance between the vegetation bands increases, suggesting that spatial distance of inhibition is proportional to t_v (Figure 2a, last column).

[13] Sensitivity analyses demonstrate the vegetation patterning which results from variable degrees of anisotropy in the hydraulic conductivities and regional hydraulic gradients (Figure 2b, selected results shown). For $k_x/k_y \leq 0.5$, the model predicts the formation of perpendicular strings for dc = 0 to 0.015 (Figure 2b). However, for dc > 0.015, and with $k_x/k_y \leq$ 0.5, homogenous distributions of plant biomass are produced. At k_x/k_y = 1, patch patterns form in the presence of small regional hydraulic gradients, while parallel string patterns form (Figure 2b, last column) in the presence of a large regional hydraulic gradient (dc = 0.025m).

4. Discussion

[14] Simulation results demonstrate that the relative magnitude of the x-y advection rates as represented through anisotropy in the regional hydraulic gradient (i.e., dc/d$y \neq 0$) or hydraulic conductivity (i.e., $k_x/k_y \neq 1$), determine the landscape-scale vegetation patterns in nutrient-limited wetland ecosystems. In the absence of anisotropy, the advection of water and dissolved nutrients towards the vegetation (local advection) are uniform in both x-y directions and results in maze patterns. In the presence of a regional hydraulic gradient, fluxes of water and dissolved nutrients flow in the direction of the gradient. When the regional advection of water and dissolved nutrients is smaller than the local advection of water and dissolved nutrients, the nutrients released from the turnover of vegetation is retained locally for growth, allowing patch patterns to form and which are maintained at steady state (Figure 2a, first three columns for $t_v > 0.7 \times 10^{-5}$ m^3 g$_B^{-1}$ day^{-1}). On the other hand, when the regional advection of water and dissolved nutrients is greater than the local fluxes, nutrients released from the turnover of vegeta-

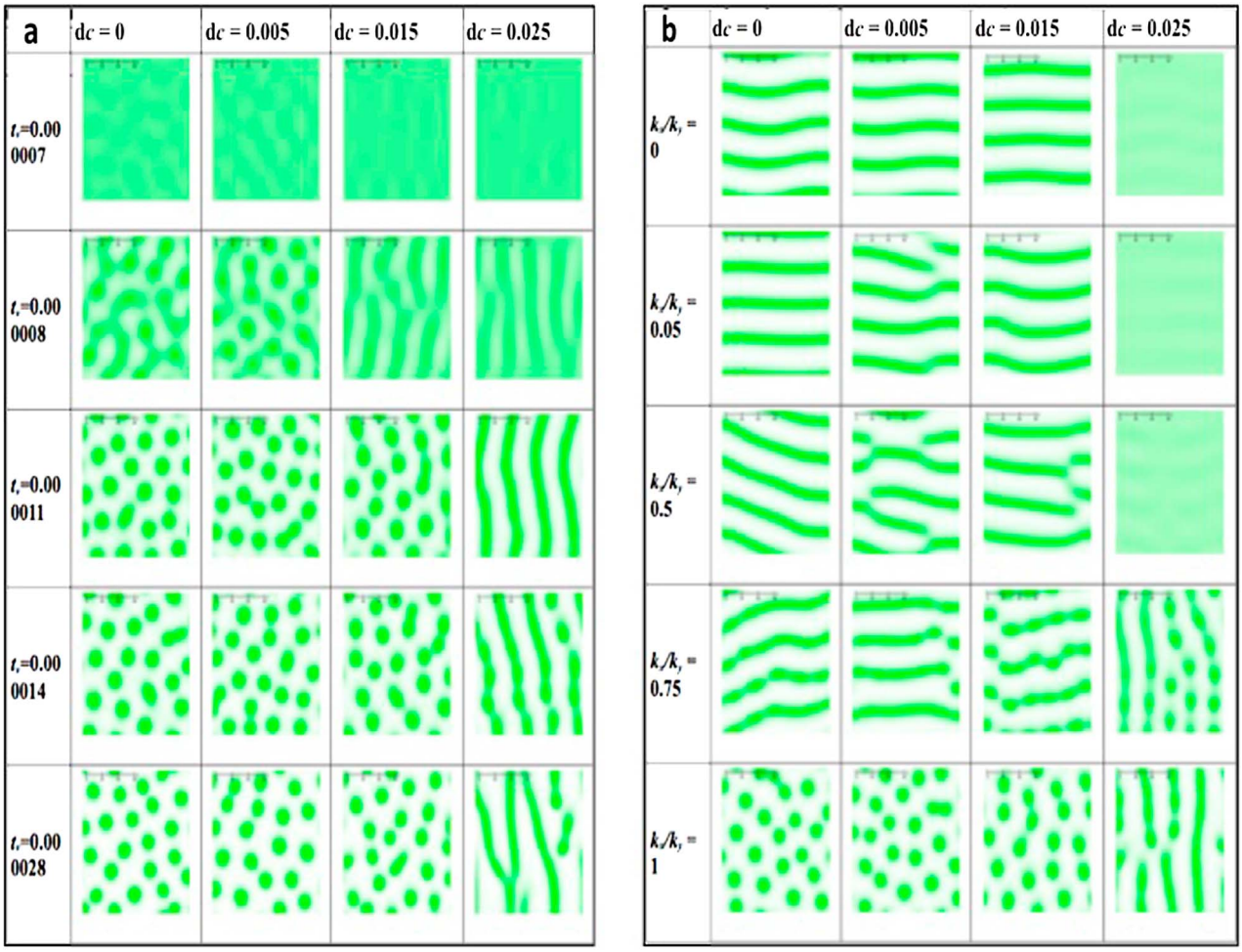

Figure 2. (a) Spatial patterns of plant biomass for $0.000007 < t_v < 0.000028$ m^3 g_B^{-1} day^{-1} and $0 < dc < 0.025$ m. (b) Spatial patterns of plant biomass for $0 < k_x/k_y < 1$ and $0 < dc < 0.025$ m.

tion are transported in the direction of the regional hydraulic gradient. For example, in the presence of a regional hydraulic gradient in the *y*-direction, the advection of water and nutrients towards vegetation in the *x*-direction inhibits the growth of perpendicular strings, while the flux of nutrients in the *y*-direction promotes the growth of parallel strings. The effect of the regional hydraulic gradient on the resulting patterns is clearly shown in the last row of Figure 2b.

[15] Simulation results suggest that the strength of the regional gradient and the effective anisotropy in hydraulic conductivities affect the resulting configuration of the vegetation pattern. In the modified Rietkerk model, the k_x/k_y ratio determines the relative strength of the long distance inhibition in the *x* and *y* directions of the domain. For example, when $k_x/k_y < 1$ and the regional hydraulic gradient in the *y*-direction is moderate (i.e., $dc < 0.015$), the advection of water and nutrients induced by transpiring vegetation in the *x*-direction is much lower than advection of water and nutrients along the longitudinal axis (*y*-direction). Biomass then grows laterally toward zones of relatively higher nutrients, and thus, perpendicular vegetation bands form. However, beyond a certain upper threshold value of the regional gradient ($dc > 0.015$), the high flux of available nutrients entering the domain in this direction and from decay in incipient vegetation patches already within the domain causes biomass to grow preferentially in the direction of the regional hydraulic gradient, and vegetation bands oriented parallel to the prevailing flow develop.

[16] The ponding mechanism as proposed by *Swanson and Grigal* [1988] induces a negative feedback between vegetation patches caused by flooding stress in the upslope direction. This negative feedback, in turn, drives the formation of perpendicular stripes. We envision that upslope ponding also results in a localized hydraulic gradient caused by the downstream resistance of the emergent vegetation, which is oriented in the direction perpendicular to the regional hydraulic gradient (*y*-direction). This then results in the advection of water and nutrients towards the patch margins, which reduces the long-distance inhibition of vegetation growth in the *x*-direction. Specifically, this advection of water and nutrients in the *x*-direction reduces the impact of the transpiration driven local hydraulic gradient in the *x*-direction. In our model, we therefore subsume the combined effects of the transpiration driven flow (explicitly represented) and the flow due to ponding (implicitly represented) into our k_x term such that $k_x/k_y < 1$. By doing so, we capture the first order effects of ponding as espoused by *Swanson and Grigal* [1988].

[17] The modeling framework proposed here differs from other modeling approaches. In a recent modeling study, *Eppinga et al.* [2009] identified three important pattern-structuring mechanisms in wetland ecosystems: peat accumulation [*Hilbert et al.*, 2000; *Belyea and Clymo*, 2001], water ponding [*Swanson and Grigal*, 1988; *Couwenberg*, 2005; *Couwenberg and Joosten*, 2005] and nutrient accumulation [*Rietkerk et al.*, 2004]. *Eppinga et al.* [2009] incorporated these processes into a single modeling framework that describes vegetation patterning as a result of interactions between four state variables: plant biomass, peat thickness, groundwater table, and nutrient availability. *Eppinga et al.* [2009] use this model to conduct a factorial analysis to explore how these mechanisms affect the resulting pattern formation. Their results suggest that nutrient accumulation alone can drive the formation of parallel strings on a slope and maze patterns on relatively flat ground, but is not sufficient to form perpendicular strings. *Eppinga et al.*'s [2009] model can only produce perpendicular string patterns when either peat accumulation or water ponding is explicitly invoked in addition to the nutrient accumulation mechanism. In another recent modeling study, *Larsen and Harvey* [2011] have demonstrated that sediment transport feedback can be an important pattern-structuring mechanism in wetland landscapes. Using a cellular automata model that describes sediment transport and vegetation dynamics, *Larsen and Harvey* [2011] have also reproduced the various vegetation patterns observed in wetland ecosystems. While we believe that both the nutrient accumulation and sediment transport feedback mechanisms are important, at present we do not yet understand the degree to which these two mechanisms operate independently or separately in patterned wetlands.

5. Conclusion

[18] We show that by representing the main effect of ponding implicitly through an effective anisotropy in hydraulic conductivity, we retain the simplicity of the original Rietkerk model and reproduce the various patterns in wetland ecosystems. Simulation results demonstrate that the relative magnitude of the x-y advection rates as represented through effective anisotropy governs pattern evolution in wetland ecosystems. We contend that the effective anisotropy in hydraulic conductivity adequately represents the mechanisms that lead to the emergence of perpendicular vegetation patterns in wetland habitats. This modeling approach thus provides an improvement in the intuitive understanding of the controls governing pattern formation in wetland ecosystems.

[19] **Acknowledgments.** This research was supported in part by the following NSF grants: 0439620, 0922100 and 1027870 as well as by a grant from the Everglades National Park (H5297-09-0011). Yiwei Cheng was additionally supported in part by an Everglades Foundation Fellowship from the Everglades Foundation.

References

Belyea, L. R. (2007), Climatic and topographic limits to the abundance of bog pools, *Hydrol. Processes*, *21*(5), 675–687, doi:10.1002/hyp.6275.

Belyea, L. R., and R. S. Clymo (2001), Feedback control of the rate of peat formation, *Proc. R. Soc. London, Ser. B*, *268*, 1315–1321, doi:10.1098/rspb.2001.1665.

Couwenberg, J. (2005), A simulation model of mire patterning—Revisited, *Ecography*, *28*, 653–661, doi:10.1111/j.2005.0906-7590.04265.x.

Couwenberg, J., and H. Joosten (2005), Self-organization in raised bog patterning: The origin of microtope zonation and mesotope diversity, *J. Ecol.*, *93*, 1238–1248, doi:10.1111/j.1365-2745.2005.01035.x.

Ellery, W. N., T. S. McCarthy, and N. D. Smith (2003), Vegetation, hydrology, and sedimentation patterns on the major distributary system of the Okavango Fan, Botswana, *Wetlands*, *23*(2), 357–375, doi:10.1672/11-20.

Eppinga, M. B., P. C. de Ruiter, M. J. Wassen, and M. Rietkerk (2009), Nutrients and hydrology indicate the driving mechanisms of peatland surface patterning, *Am. Nat.*, *173*(6), 803–818, doi:10.1086/598487.

Foster, D. R., G. A. King, P. H. Glaser, and H. E. Wright (1983), Origin of string patterns in boreal peatlands, *Nature*, *306*, 256–258, doi:10.1038/306256a0.

Hilbert, D. W., N. Roulet, and T. Moore (2000), Modelling and analysis of peatlands as dynamical systems, *J. Ecol.*, *88*, 230–242, doi:10.1046/j.1365-2745.2000.00438.x.

Larsen, L. G., and J. W. Harvey (2011), Modeling of hydroecological feedbacks predicts distinct classes of landscape pattern, process, and restoration potential in shallow aquatic ecosystems, *Geomorphology*, doi:10.1016/j.geomorph.2010.03.015, in press.

Ogden, J. C. (2005), Everglades ridge and slough conceptual ecological model, *Wetlands*, *25*(4), 810–820, doi:10.1672/0277-5212(2005)025[0810:ERASCE]2.0.CO;2.

Rietkerk, M., S. C. Dekker, M. J. Wassen, A. W. M. Verkroost, and M. F. P. Bierkens (2004), A putative mechanism for bog patterning, *Am. Nat.*, *163*(5), 699–708, doi:10.1086/383065.

Sakaguchi, Y. (1980), On the genesis of banks and hollows in peat bogs: An explanation by a thatch line theory, *Bull. Dep. Geogr. Univ. Tokyo*, *12*, 35–58.

San José, J. J., M. L. Meirelles, R. Bracho, and N. Nikonova (2001), A comparative analysis of the flooding and fire effects on the energy exchange in a wetland community (Morichal) of the Orinoco Llanos, *J. Hydrol.*, *242*(3–4), 228–254, doi:10.1016/S0022-1694(00)00392-9.

Swanson, D. K., and D. F. Grigal (1988), A simulation model of mire patterning, *Oikos*, *53*, 309–314, doi:10.2307/3565529.

Y. Cheng and M. Stieglitz, School of Civil and Environmental Engineering, Georgia Institute of Technology, 790 Atlantic Dr., Atlanta, GA 30332, USA. (gtg985z@mail.gatech.edu)

V. Engel, South Florida Natural Resources Center, Everglades National Park, 950 N. Krome Ave., Homestead, FL 33030, USA.

G. Turk, School of Interactive Computing, Georgia Institute of Technology, 85 Fifth St. NW, Atlanta, GA 30308, USA.